Modified stress and temperature-controlled direct shear apparatus on soil-geosynthetics interfaces

Zhiming Chao[1], Gary Fowmes[1]*

1.School of Engineering, University of Warwick, CV4 7AL, UK.

** Corresponding Author, email: Z.Chao@warwick.ac.uk，telephone：+44（0）7955368672, fax number: +44 (0)24 7641 8922*

Abstract: In this paper, a bespoke stress and temperature controlled direct shear apparatus to test soil-geosynthetics interfaces is introduced. By adopting the apparatus, a series of 'rapid loading' shear tests and creep tests were conducted on the Clay – Geosynthetic Drainage layer (GDL) interfaces to assess the functionality of the apparatus. The experimental results indicate that, the modified apparatus can allow the shear deformation behaviour of soil-geosynthetics interfaces under environmental stress during thermal and drying-wetting cycles to be investigated, with a reliable performance. The resistance of Clay-GDL interfaces to shear deformation under the rapid loading of shear stress decreases after drying-wetting cycle and at elevated temperature. In the creep tests, the interfaces subjected to drying-wetting cycles and thermal cycles fail under a lower shear stress level than that of the interfaces without experiencing drying-wetting cycles and thermal cycles, respectively. The impacts of drying cycles on the horizontal displacement is significantly larger than that of wetting cycles. The first drying cycle has the largest impacts on the horizontal displacement than those of the following drying cycles. The impacts of drying alone on the horizontal displacement of Clay-GDL interfaces during drying cycles are small, and the main influence factor is the elevated temperature.

Keywords: Geosynthetic interfaces; creep test; geocomposite drainage layers; drying-wetting cycle; modified direct shear apparatus; rapid loading shear test

1 Introduction

For geosynthetics-reinforced soil structures, the stability is mainly governed by the interface characteristics between soil and geosynthetics (Datta, 2010). In general, the usage of geosynthetics usually requires a minimum guaranteed service life of 10's of years. In the service life, the soil-geosynthetics interfaces can experience long-term or short-term shear deformation due to constant or increasing shear stresses, respectively, which may cause the failure of the soil-geosynthetics interfaces and impact the stability of engineering projects (Benson et al., 2012).

The displacement-controlled direct test is the most widely adopted approach to research the mechanical behaviour of soil-geosynthetics interfaces (Abu-Farsakh et al., 2007; Ferreira et al., 2015; Lee and Manjunath, 2000; Liu et al., 2009). However, the displacement-controlled direct shear test is not representative of the real situation in engineering applications because, in real project site, the shear deformation of soil-geosynthetics interfaces is controlled by stress rather than displacement (Müller et al., 2008). Additionally, displacement-controlled direct shear testing does not simulate the long-term field situation under which thermal cycle and drying-wetting cycle can impact the mechanical behaviour of soil-geosynthetics interfaces (Ghazizadeh and Bareither, 2018; Zanzinger and Saathoff, 2012). More importantly, it is impossible for the displacement-controlled direct shear apparatus to conduct creep tests on soil-

geosynthetics interfaces (Fox and Stark, 2015). Therefore, it is necessary to develop a temperature and stress-controlled direct shear apparatus that can conduct creep tests/rapid loading shear tests on soil-geosynthetics interfaces during/after thermal and drying-wetting cycles.

The soil-geosynthetics interfaces in waste containment facilities, such as landfill, are exposed to elevated temperature due to exothermal reaction from waste degradation (Abuel-Naga and Bouazza, 2013; Ishimori and Katsumi, 2012; Singh and Bouazza, 2013). For example, the temperature inside landfills are often in the range of 30 ℃ to 60 ℃ (Abuel-Naga and Bouazza, 2013; Hanson et al., 2015; Jafari et al., 2014). Due to the presence of thermo-softening plastics in geosynthetics, exposure to the elevated temperature can reduce the mechanical properties of soil-geosynthetics interfaces, such as shear strength (Bouazza et al., 2011). In addition to the elevated temperature, seasonal fluctuations, exacerbated by climate change, also has influences on its mechanical properties during the long-term behaviour of landfills (Hosney and Rowe, 2013). This is because, in general, the thickness of cover soil for landfills is relatively small (about 0.5 m to 2 m), thus is susceptible to drying-wetting cycles through its full thickness (McCartney and Zornberg, 2010). Additionally, the high temperature inside landfills further accelerates the evaporation of water in the cover soil-geosynthetics interfaces during the drying cycle, forming obvious drying-wetting cycles on the cover soil-geosynthetics interfaces during climate change and causing potential safety hazards on their long-term operation (Li et al., 2016).

Currently, the studies about the impacts of drying-wetting cycles on the mechanical properties of soil and geosynthetics under stress states, respectively, have been conducted by some researchers (Fleureau et al., 2002; Guan et al., 2010; Zhang et al., 2015). The research results

show that a drying-wetting cycle is a vital factor to influence the mechanical behaviour of soil and geosynthetics, respectively, which controls their mechanical strength (Guney et al., 2007; Md et al., 2016; Wang et al., 2016). However, due to the limitation of experimental apparatus, the influences of drying-wetting cycles on the mechanical behaviour of soil-geosynthetics interfaces under environmental stresses has not been widely researched.

The purpose of the paper is to introduce a bespoke stress and temperature-controlled large shear apparatus on soil-geosynthetics interfaces. The modified apparatus allows the shear deformation behaviour of soil-geosynthetics interfaces under environmental stress during thermal and drying-wetting cycles to be investigated. By using the apparatus, a series of rapid loading shear tests and creep tests on Clay-Geosynthetics Drainage Layer (GDL) interfaces were conducted to validate the performance of the modified apparatus. Also, the experimental results from the bespoke apparatus were compared with the results from the conventional displacement-controlled equipment to support the results.

2 Development of the temperature and stress-controlled direct shear apparatus

The schematic of the temperature and stress-controlled direct shear apparatus developed in this study is shown in Figure 1. The direct shear apparatus consists of four primary systems: normal stress system, shear stress system, heating system, and data acquisition and control system. The normal stress system comprises an air-pressure bladder which applies the normal stress via a loading plate into the soil in the upper box. The detailed description of other components is detailed below.

2.1 *Shear stress system*

The shear stress system consists of top and bottom shear boxes, pyramid teeth gripping plate (Allen and Fox, 2007), shear rods, clamping bar, loading plate, steel wires, pulleys and hanger for dead weights, as shown in Figure.1. During the shear process, the top shear box with internal dimension 300 mm in width by 300 mm in length by 100mm in height is fixed to the side walls of the direct shear apparatus. The bottom shear box with internal dimension 300 mm in width by 400 mm in length by 100 mm in height is housed in a water bath. The lower box assembly is connected to the shear rod, which is free to move horizontally through the bearing rail underneath the bottom shear box. A pulley system is connected to the end of the shear rod by using a hook. During the tests, dead weights were added to the hanger to impose stress on the bottom shear box.

In this device, a clamping bar and pyramid-teeth gripping plate are adopted to grip geosynthetics. The clamping bar is on the leading edge of the bottom shear box to clamp the geosynthetics to the bottom shear box. The pyramid-teeth gripping plate is machined on the upward surface of the aluminium heater plate. The height of the pyramid-teeth is 4 mm, and the angle of the tip of the pyramid-teeth is 60°. The width and length of the pyramid-teeth are 3 mm and 4 mm, respectively. During the tests, the sharp tips of the pyramid-teeth are penetrated into the geosynthetics to resist the relative displacement between the geosynthetics and the bottom shear box.

2.2 *Heating system*

The heating system for the direct shear apparatus consists of an aluminium lower block with an internal heating mat, Type-T thermocouple controlled using a PID temperature controller.

The heater mat is the heat source, 200 mm in length by 300 mm in width, supply voltage 240 v ac, peak temperature of 300 ℃, and power rating 240 W and is housed inside the aluminium heating plate. The aluminium heating plate is placed in the bottom shear box underneath the soil-geosynthetics interface. The aluminium heating plate is composed of separable upper and the bottom parts with width 300 mm by length 400 mm by height 20 mm and width 300 mm by length 400 mm by height 30 mm, respectively, which is fixed together by fastening the counter bore screw in the 8 counter bore holes around the circumference of heating plate. The upward surface of the upper part is machined to pyramid teeth gripping, and the downward surface is adhered to the heater mat. Meanwhile, for placing the heat mat, there is a groove with 200 mm in length by 300 mm in width by 20 mm in height in the bottom part. The temperature of the heater mat is controlled by the PID temperature controller by adjusting the voltage of the power line connected to the heater mat based on the signal from the K-type thermocouple.

There are three reasons for heating the soil-geosynthetics interfaces from under the geosynthetics. The first one is that, during the tests, normal stress was imposed from the top of the soil sample. If the heating system was installed on the top of soil layer, the distribution of normal stress in soil sample may be influenced to cause deviations in the experimental results. Secondly, if the heating system was installed on the top of soil layer, it needs to take a long time to transfer heat to the soil-geosynthetics interfaces to reach the target temperature, which may result in the insufficient drying on the interfaces due to the limitation of experimental time. However, the main aim of this apparatus is to explore the mechanical properties of soil-geosynthetics interface subjected to drying-wetting cycles, thus, heating the interfaces from the bottom can allow the temperature of soil-geosynthetics interfaces to quickly reach the target value to sufficiently dry the interfaces. Thirdly, to the best knowledge of the authors, in some

landfills, the measured temperature of cover systems is higher than the ambient temperature due to elevated temperature of the underlying wastes, and the prevailing direction of heat flow in the cover systems is upward.

Preliminary heating tests were carried out to evaluate the performance of the heating system. In order to simulate the real experiments, during the testing, the heating of soil-geosynthetics interfaces was initiated after consolidation for 24 hours under a target temperature of 40 ℃. Then, the interface was heated for 1000 minutes under the same target temperature. After that, three repetitive tests were conducted under the same target temperature to evaluate the repeatability of the heating system. During the tests, the thermocouple was placed in the drainage core of the GDL to measure the temperature of interface. Thus, the measured temperature from the thermocouple represents the actual temperature of soil-GDL interfaces. The measured temperature in elapsed time of the three tests was shown in Figure 2.

Based on Figure 2, it can be seen that, the variation trends of the three curves are similar in elapsed time, especially after they reach the target temperature. It demonstrates that the heating system has satisfied repeatability. More specifically, for the three curves, initially all rise rapidly over the target temperature. Then, they decrease gradually to the target temperature. The lag times for the three tests are all less than 200 minutes. In this paper, in the formal experiments, the heating duration is 24 hours, which is significantly higher than the lag time. Hence, the temperature equilibration ability for the heating system is acceptable. Additionally, it should be noticed that after the lag time, the temperatures of the three tests all maintain a consistent 40 ℃. Although there are some fluctuations around the targeted temperature, the fluctuations are negligible, less than 0.3 ℃.

2.3 *Data acquisition and control system*

The data acquisition and control system consists of horizontal displacement transducer, normal stress gauge, T-type thermocouple, load cell, PID temperature controller, and shear stress and horizontal displacement gauges. The horizontal displacement of the bottom shear box is measured via a single 100 mm linear potentiometer positioned at the front of the bottom shear box, as shown in Figure 1. Horizontal shear load is measured using an S-type load cell with load capacity of 4 kN. The hermetically sealed tip insulated Type-T thermocouple and the PID temperature controller are adopted to monitor and control the temperature of the soil-geosynthetics interface. The normal stress is measured and displayed via the mechanical normal stress dial.

2.4 *Type of tests*

Whilst strain controlled testing can give the strength of an interface, it does not allow the in situ conditions to be applied whilst other environmental factors are altered, whereas the stress controlled apparatus presented in this paper facilitates this. The modified apparatus can allow stress-controlled direct shear tests to be conducted on soil- geosynthetics interfaces, which can be classified as i) rapid loading shear tests or ii) creep tests. In rapid loading shear tests, shear load is continually increased until the soil-geosynthetics interface fails. In the creep tests, the soil-geosynthetics interface is subjected to constant shear stress until the soil-geosynthetics interface fails or the test is terminated. The apparatus can be utilized to carry out the rapid loading shear tests and creep tests under different temperature, or antecedent wetting-drying cycles. Additionally, in order to replicate the real *in situ* conditions, such as, climate change, the apparatus also allows soil-geosynthetics interfaces to conduct creep tests; or rapid loading shear tests during or after drying-wetting cycles/thermal cycles. These are achieved by

submerging the interfaces in water and drying them with high temperature to simulate the process of wetting-drying cycles/ thermal cycles, respectively.

3 Experimental Materials

3.1 *Test materials*

In this paper, the tests were carried out on the interface between a Mercia Mudstone (Clay) and the upper non-woven needle punched geotextile of a proprietary Geocomposite Pozidrain 6S250D/NW8. The GDL is composed of a single cuspate HDPE (High Density Polyethylene) drainage core with a medium weight Non-woven needle-punched and heat-treated staple fibre polypropylene geotextile filter thermally bonded on the dimple side and a lighter geotextile on the flat side, as shown in Figure 3, which is often placed underneath the cover soil in landfills for drainage application and is inevitable to be influenced by drying-wetting cycles with an elevated temperature. The properties of the GDL are presented in Table 1. The clay is sourced from a quarry in the East Midlands of the UK, which is distributed widely in the UK. The clay is classified as CL according to BS5930, the basic properties of the Mercia Mudstone as shown in Table 2.

Clay-GDL interfaces are often located in the cover systems of waste containment facilities. In the UK, the traditional cover system of waste containment facilities often consists of (from bottom to top) regulating layer, hydraulic barrier layer, protection layer, drainage layer, cover soil and vegetation. GDL is often adopted to act as the drainage and protection function. For the cover systems installed with GDL, their stability is mainly controlled by the mechanical properties of cover soil (clay)-GDL interfaces. If the shear resistance of clay-GDL interfaces is lower than the shear stress caused by the overlying materials, the sliding of the interfaces occurs

resulting in the failure of cover systems. Thus, researching the mechanical properties of clay-GDL interfaces is important in designing cover systems installed with GDL.

3.2 *Specimen preparation*

Test specimens were cut from a GDL roll according to recommendations in ASTM D 6072. The specimens were cut such that shearing was conducted in the machine direction. The GDL was clamped to the leading edge of the lower box. Then the upper shear box was filled with 12.29 kg of clay at optimum moisture content (11.8%) in three equal increments (25 mm height of each layer). The clay was then compacted by adopting light compaction method and each layer was compacted with 16 blows of a tamper. The total height of the clay specimen above the GDL was 75 mm with density 1.82 g/cm^3. The gap between the upper and bottom shear boxes was adjusted to maintain approximately 1mm during the testing.

During the tests, the dimple side of drainage core is upward, and the pyramid-teeth are penetrated into the geotextile bonded on the flat side of HDPE drainage core to prevent the relative movement between GDL and heating system. After tests, the geotextile bonded on the flat surface of drainage core was peeled, and the flat surface of drainage core was observed. It was found that, there was no obvious indentions in the flat side of drainage core, which indicates that the pyramid-teeth did not deeply penetrate into the drainage core and cause local elongation. Since the pyramid-teeth did not penetrate through the drainage core of GDL, the influence on the experimental results caused by the interaction between soil in upper box and the pyramid-teeth can be ignored. This can be attributed to that, in the research, the adopted normal stress is relatively low (less than 50 kPa), and the low normal stress cannot impose enough pressure to allow the pyramid-teeth to deeply penetrate into the drainage core of GDL. Additionally, after the tests, the area of GDL that was clamped by the clamping bar was

observed, and there was no elongation in the clamping area of the GDL. This may be attributed to, the adopted low normal stress results in the low peak shear strength of the soil-GDL interfaces. Thus, the maximum tensile force imposed on the GDL was small, which cannot result in obvious elongation on the GDL.

4 Experimental program and methods

4.1 *Rapid loading shear testing*

Three different types of rapid loading shear tests: standard rapid loading shear tests, tests after drying-wetting cycle, and tests at elevated temperature, were carried out under normal stress 15 kPa, 25 kPa and 50 kPa. As aforementioned, the clay-GDL interface is often used in the cover systems of waste containment facilities. In the UK, the general thickness of cover soil overlying the clay-GDL interface is 1 m to 2 m, and the normal stress on the clay-GDL interface imposed by the overlying cover soil is 20 kPa to 40 kPa. To represent the regular normal stress range imposed by the overlying cover soil, in this paper, the normal stress ranging from 15 kPa to 50 kPa is adopted, which simulates the overlying cover soil with thickness ranging from approximately 0.75 m to 2.5 m. i) Repetitive standard rapid loading shear tests, under each normal stress, were conducted after 24 hours consolidation with the clay-GDL interfaces by water, and the experimental results were used to validate the repeatability of the modified apparatus. ii) The procedure of the tests after drying-wetting cycle was that, after 24 hours consolidation, water in the external shear box was discharged and the heating system was turned on to dry the interface at a constant 40 ℃ for 24 hours. After that, a wetting process was started. The heating system was turned off, and water was poured into the external shear box to submerge the interface for 24 hours, following which the shearing stage was initiated. In this research, the rapid loading shear tests after one drying-wetting cycle were conducted under

each normal stress. iii) The process of the tests at elevated temperature was almost the same with the standard tests, except that during the whole tests, the temperature of the Clay-GDL interfaces was kept at 40 ℃ by using the heating system with submerged by water. The tests at elevated temperature were conducted under each normal stress.

The selection of 24 hours drying time is due to the following reason; During the drying process, the cover soil is also directly exposed to sunshine, which can lead to a relatively fast decrease in the moisture content of cover soil. However, in the laboratory tests, when heating from the bottom to dry the geosynthetics-clay interfaces, the falling rate of moisture content in soil may be slower. Thus, in this research, a relative long drying time of 24 hours was adopted to increase the degree of moisture content change within the soil sample. Based on the measured moisture content of soil sample after drying cycles, a significant fall of moisture content in soil sample during the drying process was observed, with about 30% less than that of the soil without experiencing drying cycles. In this case, the temperatures of the clay-GDL interfaces in cover systems of waste containment facilities are mainly controlled by two factors: the ambient temperature and the elevated temperature in the underneath waste due to the exothermal reaction of waste biodegradation and hydration. According to existing reports (Corser and Cranston, 1991), the maximum temperature of cover systems in waste containment facilities can reach up to 40 ℃. Hence, to simulate an extreme situation, in this paper, the temperature of 40 ℃ is adopted during the drying and heating cycles of the tests, respectively.

In order to further validate the reliability of the modified apparatus, the displacement-controlled direct shear tests were performed under each normal stress by using conventional displacement-controlled direct shear equipment, and the obtained experimental results were compared with the results of rapid loading shear tests. Furthermore, the peak shear strength of

the Clay - GDL interfaces under 25 kPa normal stress (17.26 kPa) obtained from the standard rapid shear tests were utilised as the reference to determine the level of shear stress in the creep tests.

The shearing of all rapid loading shear tests was conducted via adding weights at a rate of 10 kg every 5 minutes. The loading rate was determined by conducting tests with different loading rates, including 10 kg/2 min, 10 kg / 5 min,10 kg/7.5 min, 10 kg/10 min, 10 kg/15 min and 10 kg/20 min, the test results as shown in Figure 4. In Figure 4, the shear stress (kPa) has been calculated by dividing the shear load (kN) by the contact area between soil and GDL, and in this research, the contact area is 0.3 m × 0.3 m.

Based on Figure 4, the horizontal displacement at the interfaces rises gradually with the increase in shear stress until the failure of interfaces. In general, the relationship curves between horizontal displacement and shear stress for tests with different loading rates are comparable, except for the test with a rate 10 kg/ 2 min. For the tests with different loading rates from 10 kg/15 min to 10 kg/5 min, they have negligible difference in the experimental results, with similar peak shear strength of around 17 kPa. However, the peak shear strength (12 kPa) of the test with 2 minute/10 kg loading rate is significantly lower than other tests. This may be attributed to that: when 2 minute / 10 kg was adopted as the loading rate, owing to the rapid adding of dead weights, the hanger for placing dead weights was unstable, resulting in the specimen under 2 minute / 10 kg loading rate being easy to fail under the effects of hanger vibration. Since, when the shear stress loading rate ranges from 5 minute/10 kg to 15 minute/ 10 kg, the impacts of shear stress loading rate on the peak shear strength of clay-GDL interfaces can be negligible, to allow time efficient testing 10 kg/5 min was adopted as the loading rate.

It also should be noted that, unlike the experimental results of displacement-controlled tests, no distinctive peaks were observed in Figure 4 as once peak shear strength of interfaces is exceeded, failure ensues, much is the case in ultimate limit state failures in the field.

4.2 *Creep testing*

The creep tests were conducted under normal stress 25 kPa. Following 24 hours consolidation, weights were added to the hanger until the targeted shear stress was reached. In this paper, six different levels of shear stresses: 50%, 60%, 70%, 80%, 90% and 95% of the maximum peak shear strength were adopted. The peak shear strength was determined by conducting three aforementioned standard rapid loading shear tests under 25 kPa normal stress, and the average of the peak shear strength for the three tests was adopted as the reference for the creep tests.

If the horizontal displacement of Clay-GDL interfaces has not reached the maximum value (80 mm) after 4 days from imposing the shear stress by weights, drying and wetting cycles were applied to the interface. The interfaces were all initially tested submerged, the drying process was conducted before the subsequent wetting process. Water in the external shear box was discharged and the heating system was turned on to dry the interface at a constant temperature 40 ℃ for 24 hours. After that, the wetting process was carried out. The interface was fully submerged in water for 24 hours. Then, the drying cycle was conducted again. The drying-wetting cycles were repeated until the change of horizontal displacement for the Clay-GDL interface stabilised.

In order to investigate the failure mechanism of the interfaces during drying-wetting cycles and explore the individual impacts of elevated temperature on the horizontal displacement of

interfaces, creep tests during thermal cycles under shear stress levels: 70%,80% and 90% were conducted, respectively. The procedure of the creep tests during thermal cycles was almost the same with the aforementioned creep tests during drying-wetting cycles, except that during the thermal cycles, the interfaces were heated to temperature 40 ℃ whilst submerged in water. Meanwhile, to explore the individual impacts of drying on the horizontal displacement of interfaces, the creep test on Mercia Mudstone Clay-GDL interfaces subjected to drying-wetting cycle without heating under the creep shear stress level of 70 % were conducted. The procedure of the creep tests subjected to drying-wetting cycle without heating was almost the same with the creep tests subjected to drying-wetting cycles with heating, the only difference between them is that, for the creep tests subjected to drying-wetting cycles without heating, only water in the external shear box was discharged and the heating system was kept off to dry the interfaces at the room temperature of 22 ℃ for 7 days.

The wetting-drying cycles and thermal cycles are to simulate climate changes of raining/drought, and elevated temperature caused by atmospheric conditions or the biodegradation/hydration of underlying waste and ambient environment on the soil-geosynthetics interfaces, respectively. The research outcomes about the effects of wetting-drying cycles and thermal cycles on the creep behaviour of soil-geosynthetics interfaces provide references for the design of landfills in rainy areas and the landfills stored with organic wastes that can occur biodegradation and hydration, respectively. It should be noted that the focus of this paper is on the development of the apparatus.

5 EXPERIMENTAL RESULTS

5.1 Shear deformation in rapid loading shear tests

Three standard ‘rapid loading’ shear tests under normal stress 15 kPa, 25 kPa and 50 kPa, were conducted, respectively. Shear deformation versus shear stress for the tests were shown in Figure 5, respectively.

Based on Figure 5, under each normal stress, the relationship curves of horizontal displacement and shear stress for the three repetitive tests are similar, which indicates the modified apparatus has satisfied repeatability. Additionally, as expected, the peak shear strength of the interfaces rises gradually with the increase of normal stress, respectively. For example, when normal stress loading from 15 kPa to 50 kPa, the peak shear strength ascents around 81 %. It indicates that under large normal stress, the stability of the interface is stronger than that under low normal stress. Moreover, it can be seen that the failure of the Clay-GDL interfaces happened suddenly with the loading of shear stress. For instance, for the first test under 15 kPa normal stress, at around 9 kPa shear stress, the horizontal displacement is 33 mm, while in the next minute, it rises to 75 mm, indicating the failure of the interface.

With the aim to validate the modified apparatus against the results obtained from a conventional strain-controlled direct shear equipment, under different normal stresses, the average shear stress and horizontal displacement of the three repetitive rapid loading shear tests under the same shear loading time were calculated, respectively, as shown in Figure 6. Meanwhile, the experimental results of the displacement-controlled direct shear tests under normal stress 15 kPa, 25 kPa and 50 kPa were drawn in Figure 6, respectively. For stress-controlled tests, shear stress is the control variable that leads the horizontal displacement of specimens. Thus, in this paper, for the relationship curves between shear stress and horizontal displacement, shear stress is adopted as the x axis (control variable) and horizontal displacement is used as the y axis (dependent variable). In order to be consistent with the stress-

controlled tests, the horizontal displacement versus shear stress curves of displacement-controlled tests also adopts shear stress as the x axis and horizontal displacement as the y axis.

Based on Figure 6, under different normal stresses, the relationship curves between horizontal displacement and shear stress of the stress-controlled rapid loading shear tests conducted on the modified apparatus all are similar to the curves of the tests carried out on the conventional displacement-controlled direct shear equipment. For both of stress and displacement-controlled tests, based on the average peak shear strength under different normal stresses, the Mohr-Coulomb strength envelope line of the specimens was obtained, respectively, as shown in Figure 7.

Based on Figure 7, for the stress-controlled tests, the Mohr-Coulomb strength envelope line fits the experimental results well, with regression coefficient R^2 of 0.99. It indicates that the experimental results obtained from the modified apparatus conforms to the Mohr-Coulomb Criterion well. In order to further validate the reliability of the modified apparatus, two repetitive rapid loading shear tests were carried out under normal stress 20 kPa and 40 kPa, respectively, the experimental results as shown in Figure 5, and their peak shear strength was shown in Figure 7. According to Figure 7, the peak shear strength under normal stress 20 kPa and 40 kPa is close to the Mohr-Coulomb strength envelope line, and the conformity of the experimental results to the Mohr-Coulomb criterion is further validated. Additionally, the differences between the peak shear strength of the strain-controlled tests under normal stress 15 kPa, 25 kPa and 50 kPa, and the peak shear strength of the stress-controlled tests under corresponding normal stress are all within 7%, as shown in Figure 7. Moreover, based on the Mohr-Coulomb strength envelope line, the obtained cohesive force c and internal friction angle

α for the stress-controlled tests and the strain-controlled tests are close, which is 3.1 kPa and 27.7°, 3.5 kPa and 27.1°, respectively.

5.2 Impacts of drying-wetting cycle on rapid loading shear tests

In order to investigate the impacts of drying-wetting cycle on the short-term shear deformation of specimens, the rapid loading shear tests with and without drying-wetting cycle were conducted under normal stress 15 kPa, 25 kPa and 50 kPa, respectively. Figure 8 presents the relationship curves between horizontal displacement and shear stress, and horizontal displacement in elapsed time for the tests, respectively.

Based on Figure 8, horizontal displacement is always higher for those specimens subjected to a drying-wetting cycle, than those without. For example, under 25 kPa normal stress, when shear stress is 1.27 kPa at the 65^{th} minute, the horizontal displacement for the specimen after one drying-wetting cycle is 17.63 mm, while the value for the specimen without drying-wetting cycle is 11 mm. Additionally, after a drying-wetting cycle, the peak shear strength and failure time from the loading of shear stress for the interfaces decrease. For example, under 25 kPa and 50 kPa normal stress, after 1 drying-wetting cycle, the peak shear strength of soil-GDL interfaces decrease 11.91 % and 5.83 %, respectively, and the failure times reduce 15.45 % and 6.25 %, respectively, as shown in Figure 8 and Figure 9. Moreover, based on the Mohr-Coulomb strength fitting line, the cohesive force for the specimen without drying-wetting cycle is 3.2 kPa, and the internal friction angle is 27.0 °. In comparison, after the drying-wetting cycle, they reduce to 2.6 kPa and 26.1°, respectively. The above-mentioned analysis demonstrates that after drying-wetting cycle, the resistance of Clay-GDL interfaces to shear deformation under the rapid loading of shear stress decreases, which results in the fact that

Clay-GDL interface after drying-wetting cycle are easier to be failed under lower shear stress and shorter loading time than the interface without drying-wetting cycle.

5.3 Impacts of temperature on rapid loading shear tests

The rapid loading shear tests in room temperature (22 ℃) and elevated temperature (40 ℃) were performed under normal stress 15 kPa, 25 kPa and 50 kPa, respectively. Figure 10 presents the relationship curves between horizontal displacement and shear stress, and horizontal displacement in elapsed time for the tests, respectively.

Based on Figure 10, the horizontal displacement is always higher when the shearing temperature is elevated. More specifically, the difference of horizontal displacement between the specimens in room temperature and elevated temperature rises with the increase of shear stress and loading time. Additionally, in the elevated temperature, the peak shear strength and failure time of the interfaces decrease, as shown in Figure 9.

To further investigate the action mechanism of drying-wetting cycles and elevated temperature on the mechanical behaviour of the Clay-GDL interfaces, the detailed mechanism analysis was considered. The interaction mechanism of clay- GDL interfaces during rapid loading shear tests is shown in Figure 11.

As shown in Figure 11, the peak shear strength of clay-GDL interfaces is mobilised from two components: the skin friction and the interlocking effects between soil and GDL (Bacas et al., 2015). More specifically, initially, the soil specimen, nonwoven geotextile and drainage core are separate, and after the compaction during the installation of soil, soil penetrates the

geotextile and drainage core slightly. With normal stress loading, the soil and geotextile fabrics are further compressed around the drainage core and embedded into the cuspate elements of the drainage core, which enhances the interlocking effects between soil lumps and the drainage core, increasing the peak shear strength of the interface. Especially under high normal stress, a large quantity of soil and geotextile fabrics can be embedded into the drainage core under the effects of high normal stress, providing larger interlocking effects than that under low normal stress. Additionally, for the soil with high moisture saturation, it is softer and easier to be pushed into the geotextiles and drainage core compared with soil with low moisture saturation (Othman, 2016). In this research, the tests were conducted in a submerged condition with 24 hours consolidation. Although the imposed normal stress was low, the long consolidation process allowed the saturated soil to be sufficiently pressed into the geotextile and drainage core, leading to the interlocking effects being an important factor to affect the peak shear strength between soil and GDL. Figure 12 presents the surface of the soil specimens after shearing. The clear indentations caused by the cuspate elements of drainage core can be seen in the surface of the soil specimens, which indicates the considerable penetration of soil into the geotextiles and drainage core of GDL.

Due to the presence of thermo-softening plastic materials, the stiffness (modulus) of HDPE drainage core and fibers of geotextiles bonded on the drainage core decreases in elevated temperature, which results in the softening of the cuspate elements on the drainage core and the fibers of geotextiles, respectively (Hanson et al., 2015). In elevated temperature, the softening cuspate elements are easier to compress. This reduces the penetrating depth of the cuspate elements into soil, as they are easier to deform during the shearing process, weakening the interlocking effects between soil and GDL. Meanwhile, the softening fibers are easier to align during the shearing process to decrease the skin friction between soil and GDL.

Additionally, whilst likely a minor effect, the viscosity of water in soil reduces at elevated temperature, which increases the pore water pressure in soil and decreases its effective stress, causing the reduction in the strength of soil (Perkins and Sjursen, 2009). For the interfaces subjected to drying-wetting cycles, when the temperature of interfaces decreases to the normal level again, although an increase can occur in the stiffness of drainage core, the compressive deformation of the cuspate elements on the drainage core caused by elevated temperature cannot recover (Karademir, 2011). It results in the small penetrating depth of the cuspate elements into soil, weakening the interlocking effects between soil and GDL. Thus, in this research, the peak shear strength of soil-GDL interfaces subjected to drying-wetting cycles and in elevated temperature is lower than that of the original interfaces, respectively.

With regard to the decrease in the magnitude of variation between the shear stress at failure for the room temperature and at elevated temperature due to the increase in normal stress. This can be attributed to, in elevated temperature, the softening drainage core has greater flow (Chrysovergis, 2012), with an increase in the contact area between soil and GDL, enhancing the skin friction resistance, but the rising in shear strength caused by augmenting contact area is lower than the reduction in strength resulted from weakening interlocking effects between soil and GDL, thus, overall, the peak shear strength of the Clay-GDL interfaces decreases with the rise in temperature. Under high normal stress, the increasing magnitude in the contact area with the rise of temperature is higher than that under low normal stress because the drainage core has larger compressive force driving the deformation, which results in the rise in peak shear strength caused by the augmenting contact area under high normal stress being larger than that under low normal stress. Thus, overall, with the rise in temperature, the decreasing magnitude of peak shear strength under high normal stress is lower than that under low normal stress.

5.4 Impacts of the shear stress level on creep deformation

Creep tests during drying-wetting cycles were conducted on the Clay-GDL interfaces under 25 kPa normal stress with six different levels of shear stresses: 50%, 60%, 70%, 80%, 90% and 95% of the peak shear strength obtained from the standard rapid loading shear tests under 25 kPa normal stress. Figure 11 presents the shear creep deformation of specimens during the whole test.

Based on Figure 11, the level of shear stresses has large influences on the shear creep behaviour of the Clay - GDL interfaces. Horizontal displacements of the Clay-GDL interface under high shear stress level are larger than those under low shear stress level. Especially, for the specimen under 95% shear stress level, the horizontal displacement increases significantly to 79 mm before the drying-wetting cycles, indicating failure of the interface. Additionally, with the increase of shear stress, the period of the primary stage (The stage that displacement increases with diminishing displacement rate) for GDL deformation reduces. Moreover, drying-wetting cycles have larger impacts on the shear creep deformation of Clay-GDL interfaces. Before the beginning of drying-wetting cycles, after the primary creep stage, the relationship curves of horizontal displacement versus time for creep tests with shear stress level lower than 95% tend to be stable, and the change of horizontal displacement is small. However, during the first drying process, the horizontal displacement rises significantly. Especially for the shear stress levels: 90% and 80% as the first drying cycle causes the failure of the interfaces. When shear stress levels are 70%, 60%, and 50%, respectively, in the first drying process, although the horizontal displacement rises, the horizontal displacement tends to be stable in a short time and the Clay-GDL interfaces do not fail. In comparison, the following drying-wetting cycles have relatively small effects on their horizontal displacement. In order to analyse the shear creep

deformation of the specimen under 95% shear stress level in detail, the creep deformation of the specimens in the first 200 minutes was drawn in Figure 12.

Based on Figure 12, for the specimen under 95% shear stress level, in the primary stage, the horizontal displacement rises rapidly to 46 mm at 19 minutes. In the following secondary stage with 112 minutes, the specimen experiences an increase of 10 mm. Then, the interface fails suddenly in the tertiary stage of 50 minutes with the rapid rise in horizontal displacement. In total, it takes 180 minutes for the failure of the interface under 95% shear stress level. In comparison, for the specimens under low stress level (lower than 95%), after the significant rise of horizontal displacement in the primary stage, their horizontal displacement keeps stable in the secondary stage, and does not experience the tertiary stage with a sharp increase until the beginning of drying-wetting cycles. Moreover, compared with the variation trend of the horizontal displacement for the rapid loading shear test under 25 kPa normal stress in Figure 5, the variation trend of creep tests is obviously different with that of rapid loading shear tests. During the rapid loading shear test, the changing rate of the horizontal displacement rises gradually in elapsed time, and the interface fails very suddenly. It demonstrates that, compared with the creep failure of the interfaces, the rapid loading shear failure is more rapid and unanticipated.

5.5 Impacts of drying-wetting cycles on the creep behaviour

In order to further analyse the impact of drying-wetting cycles on the creep deformation of the interfaces, the beginning time of the first drying cycle was taken as the 0 minutes, and the horizontal displacement in the beginning of the first drying cycle was taken as 0 mm. The relationship curves between the horizontal displacement of Clay-GDL interfaces under 70%, 60% and 50% shear stress levels and time were drawn in Figure 13, respectively.

Based on Figure 13, the first drying cycle has the largest impact on the horizontal displacement compared with the following drying cycles. Taking the interface under 70% shear stress level as an example, the horizontal displacement rises 6 mm during the first drying cycle. In comparison, the rising magnitudes during the second and third cycles are 2 mm and 1 mm, respectively, which is about 3 times and 6 times less than that of the first one. Additionally, the drying cycle has larger impacts on the horizontal displacement than that of the wetting cycle. For example, during the first drying cycle, the rising magnitude of the horizontal displacement for the interface under 60% shear stress level is 6 mm, while during the first wetting cycle, the rising magnitude is 0.5 mm, which is approximately 12 times less than that during the first drying cycle. Meanwhile, the magnitude for the second drying cycle is 1 mm, which is about 3 times higher than that during the second wetting cycle. For the third cycle, the horizontal displacement rises 0.5 mm during the drying process, which is 2 times higher than that during the wetting process. Furthermore, under the higher shear stress level, the rising magnitude of the horizontal displacement during the drying cycle is larger than that under the low shear stress level. For example, in the first drying cycle, the horizontal displacements for the interfaces under 70%, 60% and 50% shear stress levels are 6 mm, 5.70 mm and 4.60 mm, respectively.

5.6 Impacts of thermal cycles on the creep behaviour

The above-mentioned analysis shows that, the drying cycles lead to an increase of horizontal displacement for Clay-GDL interfaces, and can induce failure of the Clay-GDL interfaces under high shear stress level. However, the mechanism of this response remains uncertain due to the fact that during the drying cycles, there are two main variables that may cause the response; Except for the drying, the elevated temperature also may result in the large deformation of the Clay-GDL interface due to the presence of thermo-softening plastics. Both

phenomena are of common occurrence in real landfill capping systems, and have significant impacts on their performance.

In order to investigate the individual influence of elevated temperature on the creep deformation of Clay-GDL interface, respectively, three creep tests during thermal cycles under shear stress level: 90%, 80% and 70% were carried out. The procedure of the creep tests during thermal cycles was almost the same with the creep tests during drying-wetting cycles, the only difference between them is that, for the creep tests during thermal cycles the interface was submerged in water, and the interface and water were heated to temperature 40 ℃ for 24 hours together. The experimental results of the creep tests during thermal cycles and the corresponding creep tests during drying-wetting cycles under the same shear stress levels were plotted in Figure 14.

Based on Figure 14, for the specimens during thermal cycles, their horizontal displacement increases significantly during the first thermal cycle due to the rise of temperature. Especially for the interfaces under shear stress level: 90% and 80%, they fail during the first thermal cycle. It indicates that the elevated temperature can lead in the obvious rise of horizontal displacement for the specimens in the creep process, which can be one of factors that result in the increasing shear creep deformation during the drying cycle in the creep tests.

In order to further determine that, during the drying cycle, the increases of shear creep deformation for the Clay-GDL interfaces is due to the combined impacts of elevated temperature and drying, or the individual impact of the two factors, respectively, the time of the first drying/thermal cycle was taken as the 0 minute, and the horizontal displacement in the beginning of the first drying/thermal cycle was taken as 0 mm. The relationship curves between

the horizontal displacement of Clay-GDL interfaces in the creep tests during thermal cycles and the creep tests during drying-wetting cycles under 70% shear stress levels and time were drawn in Figure 15, respectively.

Based on Figure 15, the rise of horizontal displacement during the thermal cycles is higher than those during the drying cycles. For example, during thermal cycles, the horizontal displacement rises 7 mm and 2.2 mm, respectively, which is around 1.4 mm and 0.20 mm higher that those during the first and second drying cycles respectively. Additionally, it should be noted that, for the specimens in the creep tests during thermal cycles, the increase of horizontal displacement during the wetting cycles is larger than those of the specimens in the creep tests during the drying-wetting cycles. This can be explained that, in the wetting cycles of the creep tests during thermal cycles, although the heating system of the apparatus is stopped, due to the high temperature of water, the time for the interface and water to cool to room temperature is obviously longer than that in the creep tests during drying-wetting cycles. Thus, with a high temperature, the horizontal displacement of the specimens during the wetting cycles in the creep tests during thermal cycles is larger than that in the creep tests during drying-wetting cycles.

5.7 Impacts of drying-wetting cycle without heating on the creep behaviour

In order to further investigate the individual influence of drying on the creep deformation of the soil-GDL interface, respectively, the creep test on Mercia Mudstone Clay-GDL interfaces subjected to drying-wetting cycle without heating under the creep shear stress level of 70 % of peak were conducted. The procedure of the creep tests subjected to drying-wetting cycle without heating was almost the same with the creep tests subjected to drying-wetting cycles, the only difference between them is that, for the creep tests subjected to drying-wetting cycles

without heating, only water in the external shear box was discharged and the heating system was not used to dry the interfaces, which thus remained at the room temperature of 22 ℃ for 7 days. The experimental results of the creep tests on Mercia Mudstone Clay-GDL interfaces subjected to drying-wetting cycle without heating and the corresponding creep tests subjected to drying-wetting cycles and thermal cycles, respectively, under the same creep shear stress level, were plotted in Figure 18.

Based on Figure 18, for the Clay-GDL interface subjected to drying cycle without heating, its horizontal displacement remains stable during the drying process without heating. The variation in the horizontal displacement of the interfaces during the drying cycles with heating and the heating processes of thermal cycles is significantly higher than during the drying cycle without heating, respectively. It indicates that the drying alone does not lead to an apparent rise of horizontal displacement for Clay-GDL interfaces during creep deformation, and has a small contribution to the increase in shear creep deformation during the drying cycles with heating in the creep tests.

In order to further determine that, during the drying cycles, the increase in creep shear deformation of Clay-GDL interfaces is due to the combined impacts of elevated temperature and drying, or the individual impacts of the two factors, taking the beginning time of the first drying cycle without heating as the 0 minute, and the horizontal displacement at the beginning of the first drying cycle without heating as 0 mm, the horizontal displacement of Clay-GDL interfaces subjected to drying-wetting cycle without heating under the creep shear stress level of 70 % in elapsed time were plotted in Figure 17.

As shown in Figure 17, the rise of horizontal displacement during the drying cycle without heating is significantly lower than those during the drying cycles with heating and heating processes of thermal cycles, respectively. Regarding the specific variation amplitude of horizontal displacement, the horizontal displacement rises 0.4 mm during the drying cycle without heating, while the value for the first heating process of thermal cycles and the first drying cycle with heating is 6.8 mm and 6.1 mm, respectively. It indicates that the impacts of drying alone on the rise in the horizontal displacement of Clay-GDL interfaces during drying cycles with heating are marginal, and the main influence factor is the elevated temperature.

To further investigate the action mechanism of drying-wetting cycles, thermal cycles, and drying-wetting cycles without heating on the creep deformation of the Clay-GDL interfaces, the detailed mechanism analysis was conducted. As shown in Section 5.3, the peak shear strength of clay-GDL interfaces is mobilised from two components: the skin friction and the interlocking effects between soil and GDL (Bacas et al., 2015). The creep shear resistance between soil and GDL can also be attributed to the skin friction and interlocking effects between soil and GDL, as shown in Figure 9.2. In this research, the adopted normal stress in the creep tests is 25 kPa, and as with the rapid loading shear tests, before imposing shear stress in the creep tests, the interfaces were subjected to 24 hours consolidation time whilst submerged by water. Although the imposed normal stress was not very high, the long consolidation process allowed saturated soil to be sufficiently pressed into the geotextile and drainage core of GDL, leading to the interlocking effects as an important factor to influence the creep shear resistance between soil and GDL.

As mentioned in Section 5.3, regarding the presence of thermoplastic materials, the stiffness (modulus) of HDPE drainage core and fibers of geotextiles bonded on the drainage core

decreases at elevated temperature, which results in the softening of the cuspate elements on the drainage core and the fibers of geotextiles to weaken the interlocking effects and skin friction between soil and GDL, respectively. Additionally, at elevated temperature, the viscosity of water in soil reduces, which increases the pore water pressure in soil to decrease its effective stress, causing the decline in the shear strength of soil. Thus, in this research, during drying cycles and heating cycles, the creep deformation of clay-GDL interfaces rises because of the decreasing creep shear resistance caused by the elevated temperature. When the temperature of the HDPE drainage core decreases to the normal level again, an increase can occur in the stiffness of the cuspate elements on drainage core and the fibers of geotextiles, which results in the rise in the interlocking effects and skin friction between soil and GDL, respectively. The higher impacts of the first drying cycle and heating cycle on the creep deformation of clay-GDL interfaces than those of the following drying cycles and heating cycles can be ascribed to that, after the first drying cycle and heating cycle, even though the temperature decreases to the normal level, the interlocking effects and skin friction of the interfaces cannot fully rise to the original level before the increase in temperature, respectively, because the compressive deformation of the cuspate elements caused by elevated temperature cannot recover and the aligned fibers caused by elevated temperature cannot return to the original state. Thus, after experiencing the elevated temperature in the first drying cycle and heating cycle, before imposing the following drying cycles and heating cycles, the interlocking effects and skin friction of the interfaces are already lower than the original level. During the following drying cycles and heating cycles, at elevated temperature, when the interlocking effects and skin friction of the interfaces decrease to the same level with that in the first drying cycle and heating cycle, the decreasing magnitude is lower than those during the first drying cycle and heating cycle which results in the rise in the horizontal displacement of clay-GDL interfaces during the first drying cycle and heating cycle is higher than those during the following drying cycles and

heating cycles. Moreover, the higher creep deformation during heating cycles than that of drying cycles can be attributed to the existence of water. During the heating cycles, the clay-GDL interfaces were submerged by water. As aforementioned, the added water can soften the overlying soil sample, dissolving the cement between soil particles, which provides more lubrication between soil particles and clay-GDL interface, decreasing the shear strength of clay-GDL interfaces. In comparison, during the drying cycles, the overlying soil sample is unsaturated, which leads to the generation of suction to enhance the shear strength of clay-GDL interfaces.

The variation in the horizontal displacement of interfaces during the drying cycles and the heating processes of thermal cycles is significantly higher than that during the drying cycle without heating. It can be attributed to that, at the room temperature, the stiffness (modulus) of the cuspate elements on HDPE drainage core and the fibers of geotextiles keeps stable, which does not result in the softening of the cuspate elements and fibers to weaken the interlocking effects and skin friction between soil and GDL. Additionally, at the room temperature, the viscosity of water in soil specimens keeps stable, which does not increase the pore water pressure in the soil and decrease its effective stress, without experiencing the decrease in the shear strength of soil. Thus, in this research, during drying cycles without heating, the variation in creep deformation of clay-GDL interfaces is significantly lower than that during the drying cycles with heating and heating processes in the thermal cycles.

6. CONCLUSION

In this paper, a temperature and stress-controlled direct shear apparatus was developed. By adopting this apparatus, a series of rapid loading shear tests and creep tests were conducted on the Clay – GDL interfaces to validate the performance of the modified apparatus. Based on the

experimental results, the impacts of shear stress level, temperature, thermal cycles, and drying-wetting cycles on the rapid loading shear deformation and creep deformation of the Clay- GDL interfaces were investigated. The main conclusions are summarised as follows.

1. The performance of the modified temperature and stress-controlled direct shear apparatus was validated by carrying out repetitive tests and comparing with the displacement-controlled experimental results.

2. The resistance of Clay-GDL interfaces to shear deformation under the rapid loading of shear stress decreases after drying-wetting cycle and at elevated temperatures.

3. In the creep tests, the Clay-GDL interfaces subjected to drying-wetting cycles and thermal cycles fail under a lower shear stress level than that of the interfaces without experiencing drying-wetting cycles and thermal cycles, respectively.

4. In the creep tests, the impacts of drying cycles on the horizontal displacement of the Clay-GDL interfaces are significantly larger than that of wetting cycles. Among the drying cycles, the first cycle has the largest impacts on the horizontal displacement than that of the following cycles.

5. The elevated temperature also can lead to the obvious rise of horizontal displacement for the specimens in the creep process. During the thermal cycle, the increases of shear creep deformation for the Clay-GDL interfaces is higher than those during the drying cycles.

6. The impacts of drying alone on the rise in the horizontal displacement of Clay-GDL

interfaces during drying cycles are marginal, and the main influence factor is the elevated temperature.

7. Unlike in strain-controlled testing, the stress-controlled apparatus allows in situ stress conditions to be applied (and varied if required) whilst other environmental conditions (temperature and saturation conditions) are altered.

Acknowledgments: The authors wish to acknowledge the support from China Scholarship Council (CSC).

7. Reference

Abu-Farsakh, M., Coronel, J., Tao, M., 2007. Effect of soil moisture content and dry density on cohesive soil–geosynthetic interactions using large direct shear tests. Journal of Materials in Civil Engineering 19 (7), 540-549.

Abuel-Naga, H.M., Bouazza, A., 2013. Thermomechanical behavior of saturated geosynthetic clay liners. Journal of Geotechnical and Geoenvironmental Engineering 139(4), 539-547.

Allen, J., Fox, P., 2007. Pyramid-tooth gripping surface for GCL shear testing.In: Geosynthetics ’07. North American Geosynthetics Society, Washington, DC, pp. 1-9.

Bacas, B., Cañizal, J., Konietzky, H., 2015. Frictional behaviour of three critical geosynthetic interfaces. Geosynthetics International 22 (5), 355-365.

Benson, C.H., Edil, T.B., Wang, X., 2012. Evaluation of a final cover slide at a landfill with recirculating leachate. Geotextiles and Geomembranes 35 (9), 100-106.

Bouazza, A., Nahlawi, H., Aylward, M., 2011. In situ temperature monitoring in an organic-waste landfill cell. Journal of Geotechnical and Geoenvironmental Engineering 137 (12), 1286-1289.

Chrysovergis, T.S., 2012. Laboratory Investigation of the Effects of Temperature and Moisture on Interface Shear Strength of Textured Geomembrane and Geosynthetic Clay Liner. California Polytechnic State University, California, USA.

Corser, P., Cranston, M., 1991. Observations on the performance of composite clay liners and covers. In: Proc. Geosynthetic Design and Performance. Vancouver, Canada, pp. 59-63.

Datta, M., 2010. Factors affecting slope stability of landfill covers. In: Advances in Environmental Geotechnics. Hangzou, China, pp. 620-624.

Ferreira, F., Vieira, C.S., Lopes, M., 2015. Direct shear behaviour of residual soil–geosynthetic interfaces–influence of soil moisture content, soil density and geosynthetic type. Geosynthetics International 22 (3), 257-272.

Fleureau, J.-M., Verbrugge, J.-C., Huergo, P.J., Correia, A.G., Kheirbek-Saoud, S., 2002. Aspects of the behaviour of compacted clayey soils on drying and wetting paths. Canadian Geotechnical Journal 39(6), 1341-1357.

Fox, P.J., Stark, T.D., 2015. State-of-the-art report: GCL shear strength and its measurement–ten-year update. Geosynthetics International 22(1), 3-47.

Ghazizadeh, S., Bareither, C.A., 2018. Stress-controlled direct shear testing of geosynthetic clay liners I: Apparatus development. Geotextiles and Geomembranes 46 (5), 656-666.

Guan, G.S., Rahardjo, H., Choon, L.E., 2010. Shear strength equations for unsaturated soil under drying and wetting. Journal of Geotechnical and Geoenvironmental Engineering 136 (4), 594-606.

Guney, Y., Sari, D., Cetin, M., Tuncan, M., 2007. Impact of cyclic wetting–drying on swelling behavior of lime-stabilized soil. Building and Environment 42 (2), 681-688.

Hanson, J., Chrysovergis, T., Yesiller, N., Manheim, D., 2015. Temperature and moisture effects on GCL and textured geomembrane interface shear strength. Geosynthetics International 22 (1), 110-124.

Hosney, M., Rowe, R.K., 2013. Changes in geosynthetic clay liner (GCL) properties after 2 years in a cover over arsenic-rich tailings. Canadian Geotechnical Journal 50 (3), 326-342.

Ishimori, H., Katsumi, T., 2012. Temperature effects on the swelling capacity and barrier performance of geosynthetic clay liners permeated with sodium chloride solutions. Geotextiles and Geomembranes 33 (7), 25-33.

Jafari, N.H., Stark, T.D., Rowe, R.K., 2014. Service life of HDPE geomembranes subjected to elevated temperatures. Journal of Hazardous, Toxic, and Radioactive Waste 18 (1), 16-26.

Karademir, T., 2011. Elevated Temperature Effects on Interface Shear Behavior. Georgia Institute of Technology. Georgia, USA.

Lee, K., Manjunath, V., 2000. Soil-geotextile interface friction by direct shear tests. Canadian Geotechnical Journal 37 (1), 238-252.

Li, J., Li, L., Chen, R., Li, D., 2016. Cracking and vertical preferential flow through landfill clay liners. Engineering Geology 206 (9), 33-41.

Liu, C.-N., Ho, Y.-H., Huang, J.-W., 2009. Large scale direct shear tests of soil/PET-yarn geogrid interfaces. Geotextiles and Geomembranes 27 (1), 19-30.

McCartney, J.S., Zornberg, J.G., 2010. Effects of infiltration and evaporation on geosynthetic capillary barrier performance. Canadian Geotechnical Journal 47 (11), 1201-1213.

Md, S.H., Ling-wei, K., Song, Y., 2016. Effect of drying-wetting cycles on saturated shear strength of undisturbed residual soils. American Journal of Civil Engineering 4 (4), 143-150.

Müller, W., Jakob, I., Seeger, S., Tatzky-Gerth, R., 2008. Long-term shear strength of geosynthetic clay liners. Geotextiles and Geomembranes 26 (2), 130-144.

Othman, M., 2016. Interface Behaviour and Stability of Geocomposite Drain/Soil Systems. Loughborough University, Loughborough, UK.

Perkins, S.W., Sjursen, M., 2009. Effect of cold temperatures on properties of unfrozen Troll clay. Canadian Geotechnical Journal 46 (12), 1473-1481.

Singh, R.M., Bouazza, A., 2013. Thermal conductivity of geosynthetics. Geotextiles and Geomembranes 39 (9), 1-8.

Wang, D.-Y., Tang, C.-S., Cui, Y.-J., Shi, B., Li, J., 2016. Effects of wetting–drying cycles on soil strength profile of a silty clay in micro-penetrometer tests. Engineering Geology 206 (9), 60-70.

Zanzinger, H., Saathoff, F., 2012. Long-term internal shear strength of a reinforced GCL based on shear

creep rupture tests. Geotextiles and Geomembranes 33 (9), 43-50.

Zhang, B., Zhang, J., Sun, G., 2015. Deformation and shear strength of rockfill materials composed of soft siltstones subjected to stress, cyclical drying/wetting and temperature variations. Engineering Geology 190 (9), 87-97.

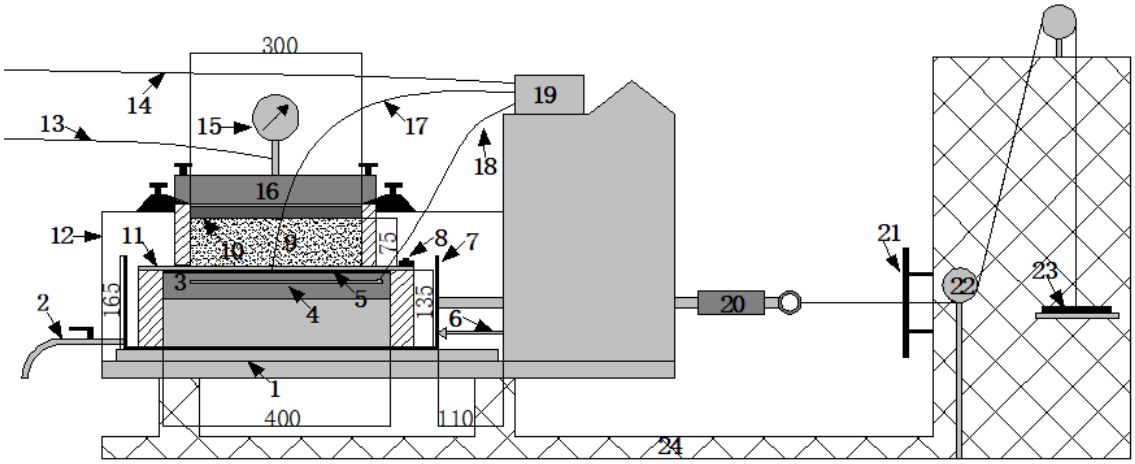

1. Bearing rail 2. Drain pipe 3. Aluminium heating plate 4. Heater mat 5. Pyramid teeth gripping plate 6. Horizontal movement transducer 7. Water bath 8. Clamping bar 9. Soil 10. Loading plate 11. Geosynthetics 12. Side walls 13. Pressurised air inlet tube 14. Main power line 15. Normal stress gauge 16. Air pressure bladder 17. Thermocouple 18. Power line to heater mat 19. PID temperature controller 20. Load cell 21. Protection plate 22. Pulley 23. Dead weight 24. Reaction frame

Figure.1 The schematic of the developed stress-controlled direct shear apparatus (mm)

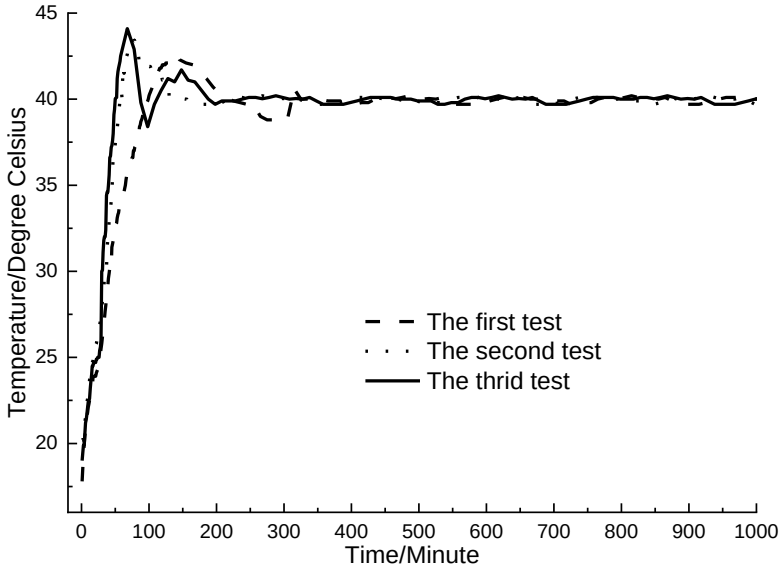

Figure.2 The measured temperature in elapsed time

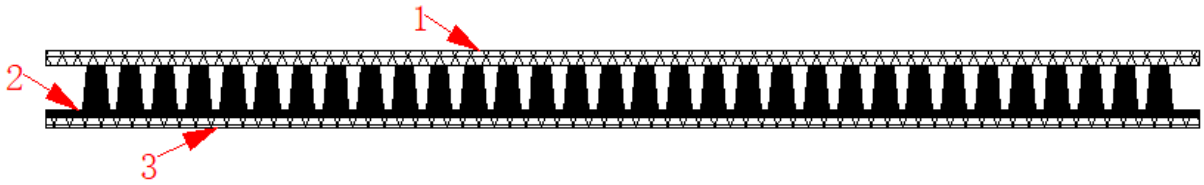

1. Geotextile boned on the dimple side 2. Drainage core 3. Geotextile bonded on the flat side

Figure.3 The schematic diagram of the GDL

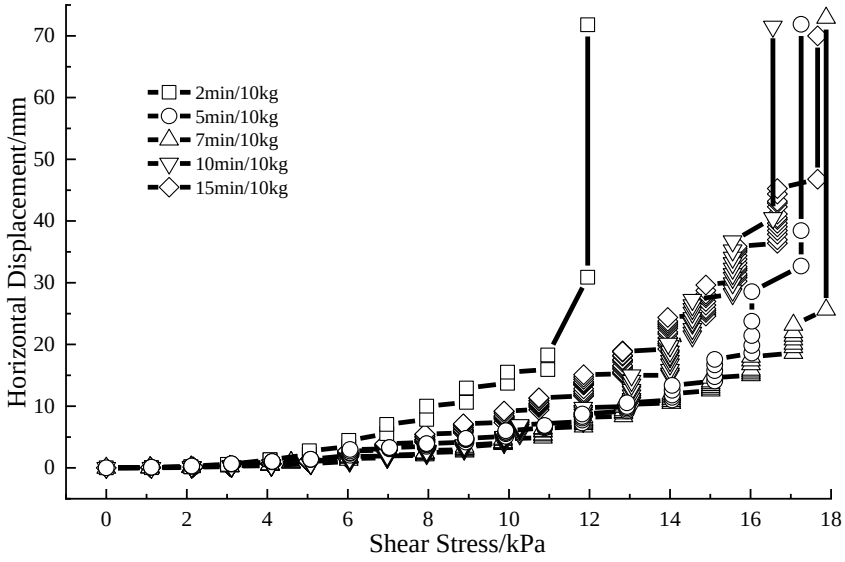

Figure.4 Experimental results for rapid loading shear tests with different loading rates

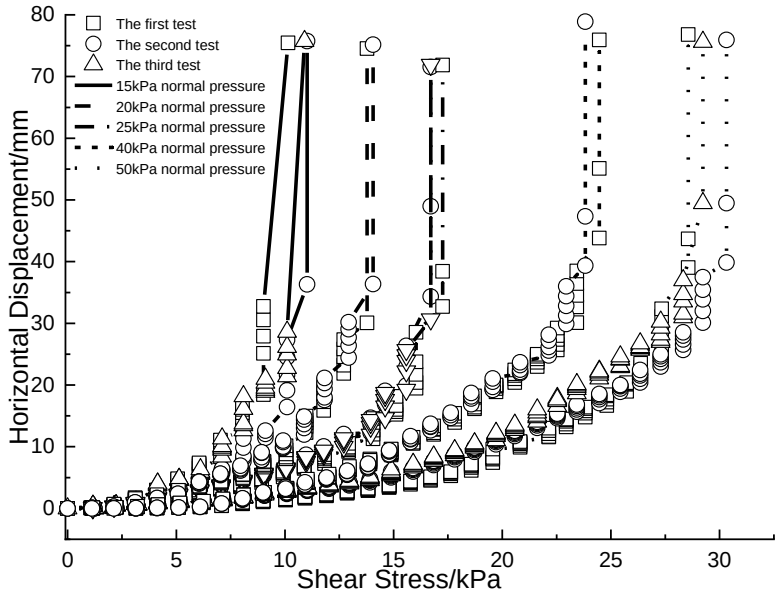

Figure.5 Experimental results of repetitive rapid shear loading tests

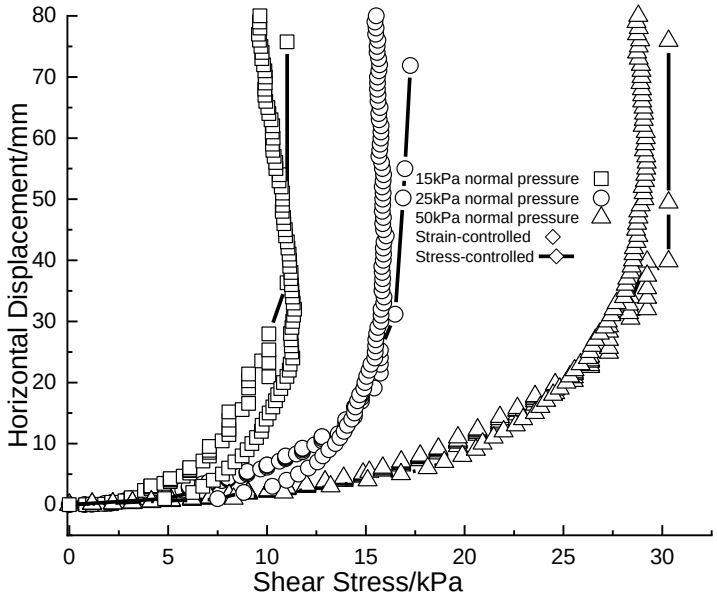

Figure.6 The comparison of stress-controlled and displacement-controlled test results

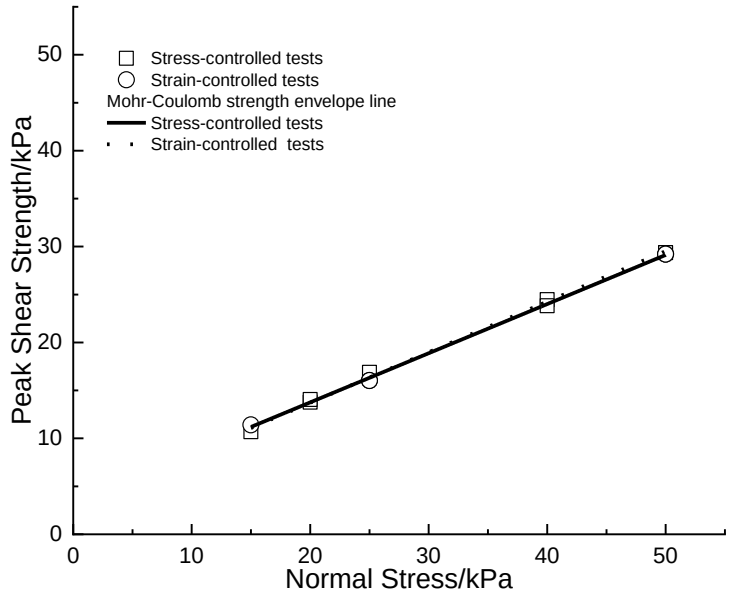

Figure.7 Mohr-Coulomb strength envelope line for repetitive rapid loading shear tests

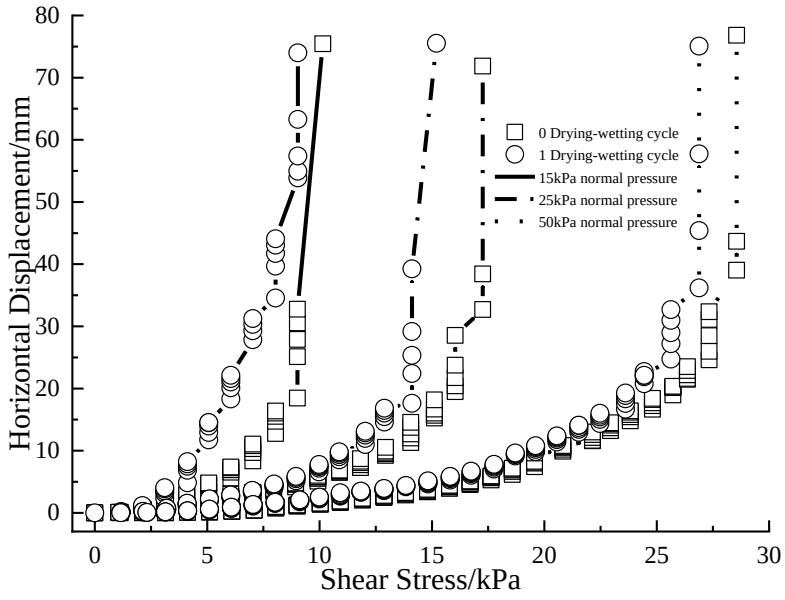

Figure.8 The experimental results of rapid loading shear tests after drying-wetting cycle

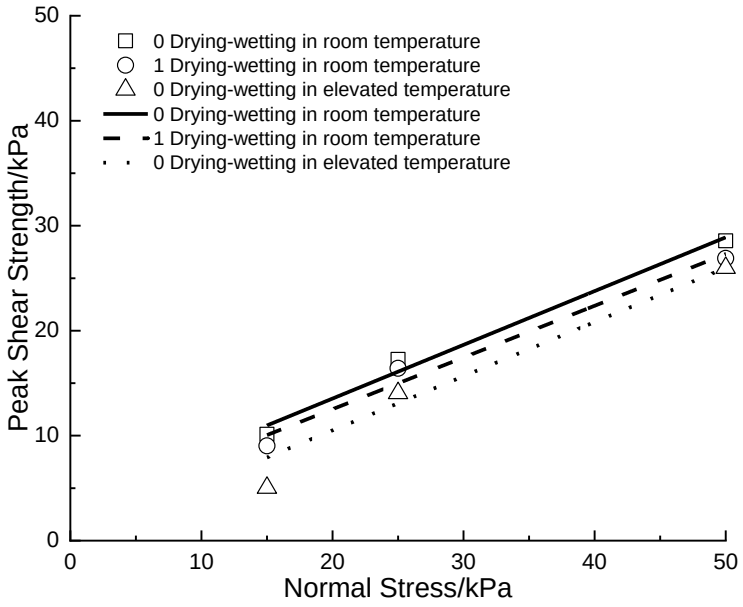

Figure.9 The impacts of drying-wetting cycle and temperature on strength envelope lines

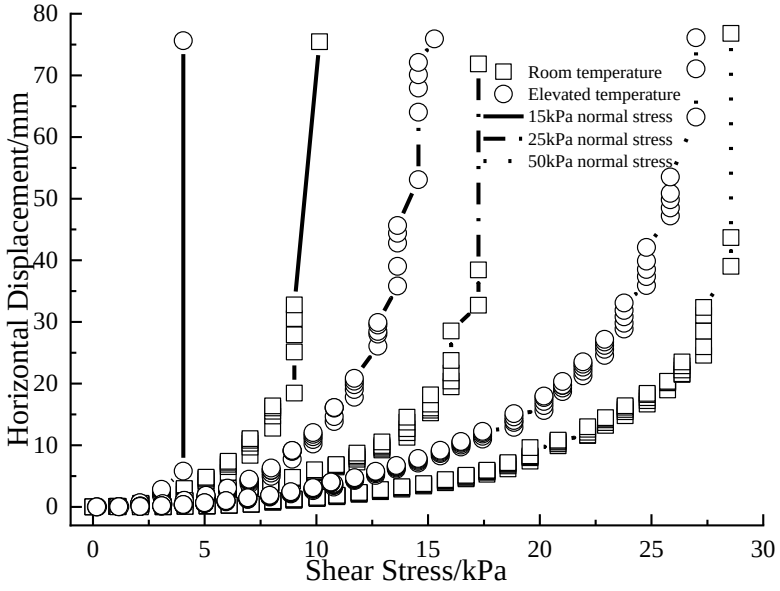

Figure.10 Experimental results of rapid loading shear tests at elevated temperature

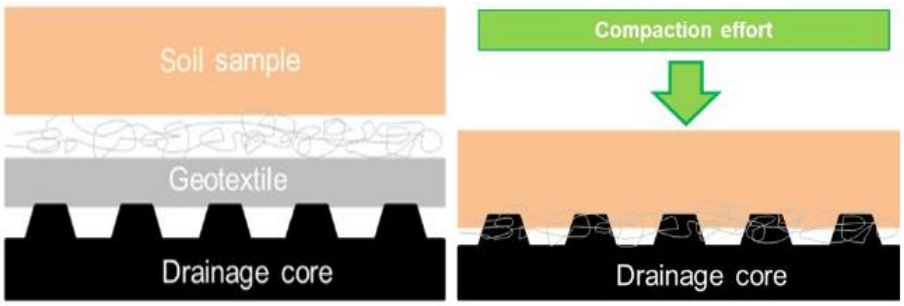

(a) Original state (b) After compaction

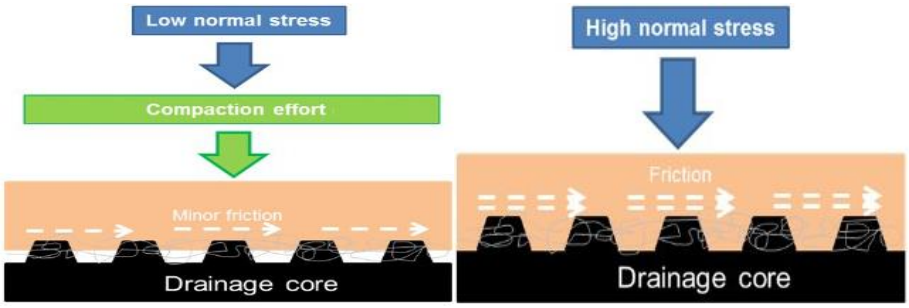

(c) Under low normal stress (d) Under high normal stress

Figure.11 The interaction mechanism between clay and GDL

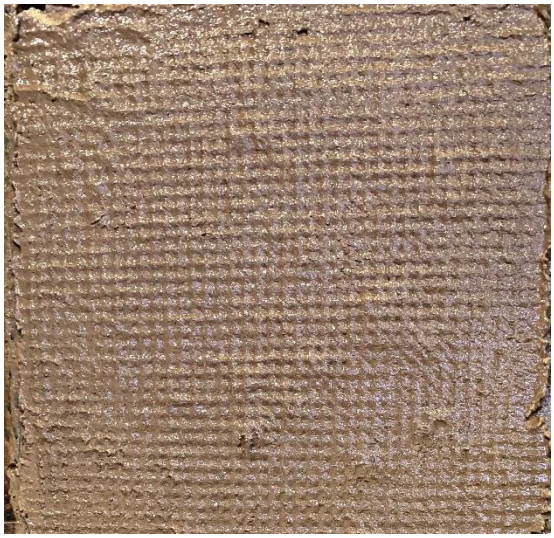

Figure.12 The surface of Clay after shearing

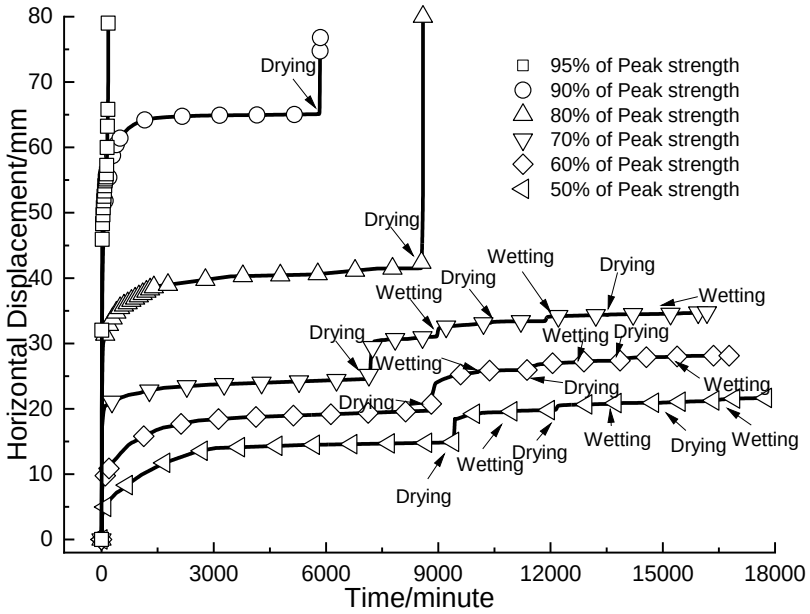

Figure.13 The shear creep deformation during the whole test

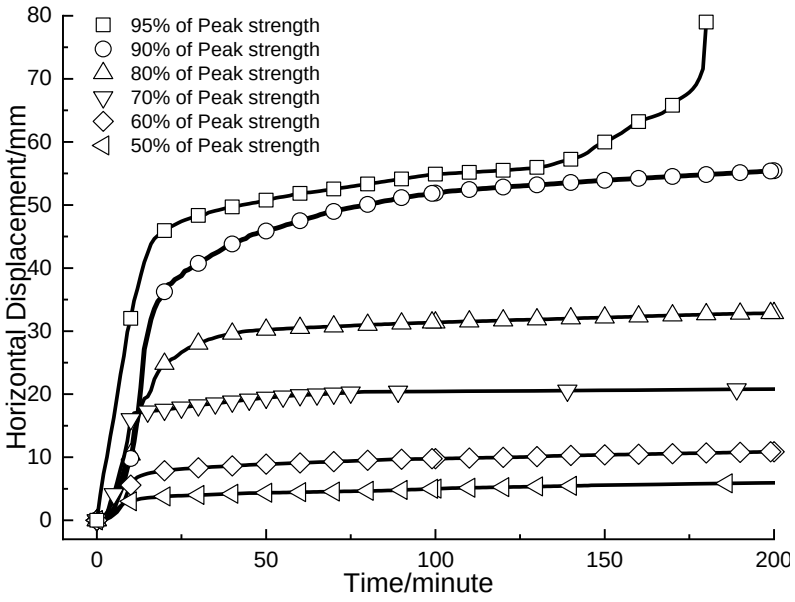

Figure.14 The shear creep deformation during the first 200 minutes

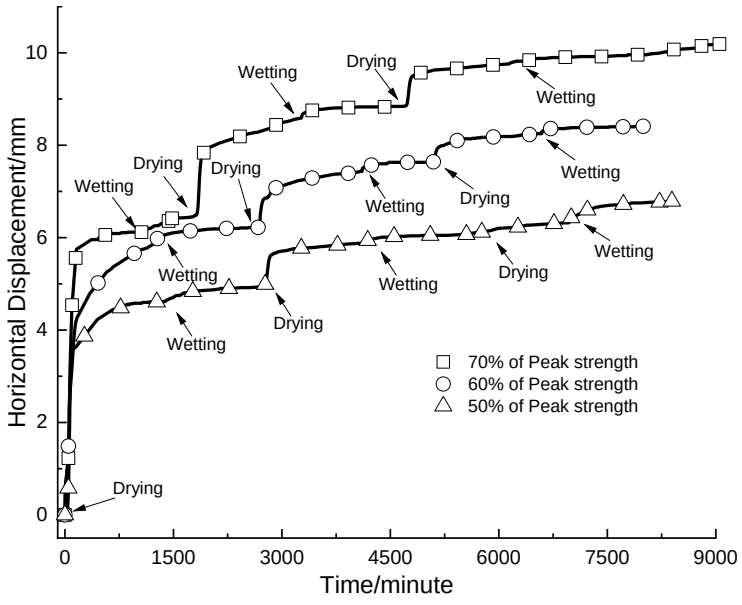

Figure.15 The shear creep behaviour during drying-wetting cycles

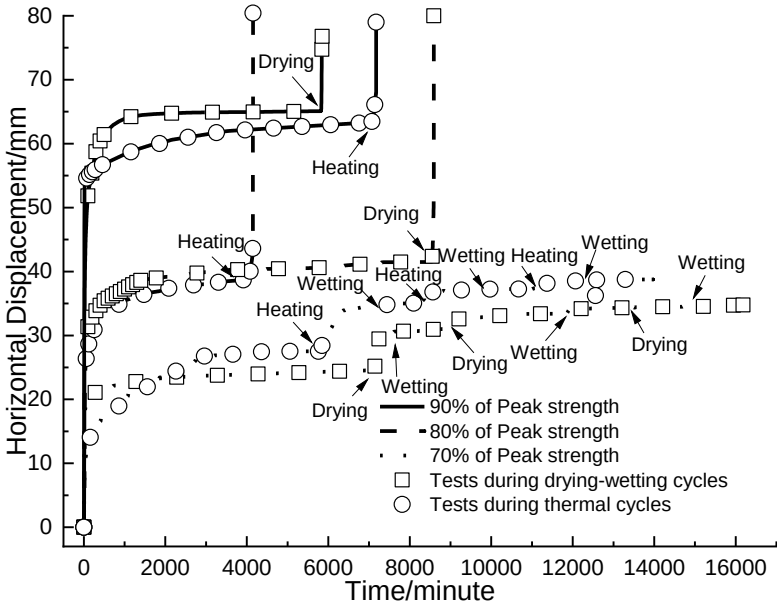

Figure.16 The influence of thermal cycles on creep behaviour during the whole tests

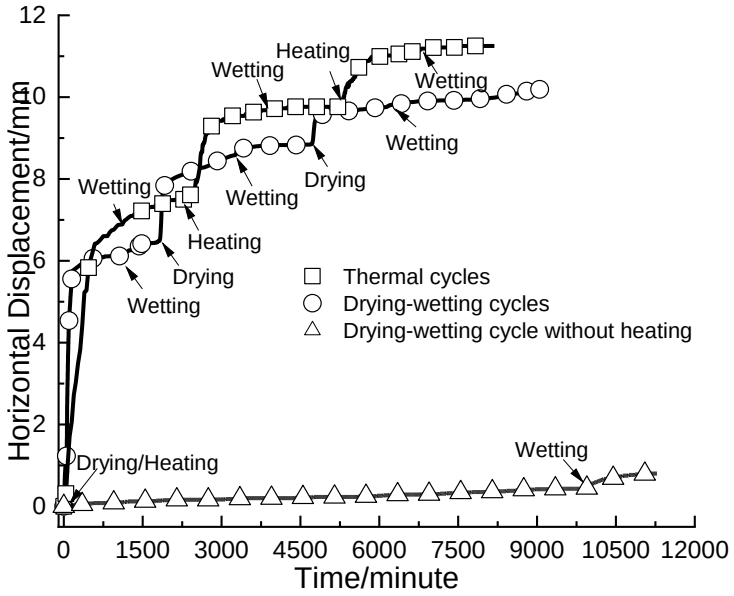

Figure.17 The impacts of thermal cycles and drying-wetting cycle without heating on the creep deformation

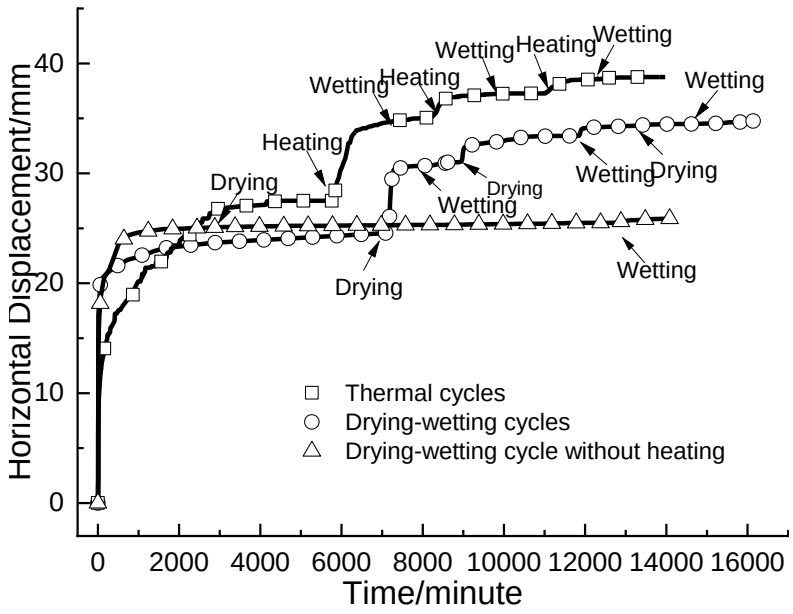

Figure.18 The influence of drying-wetting cycle without heating on creep behaviour of Clay-GDL interfaces during the whole tests

Table.1 The properties of Geocomposite Drainage Layer

GDL properties	GDL	
Thickness of drainage core at 2kPa (mm)	6	
Drainage core type	Single direction cuspate core	
Mass per unit area (g/m²)	840	
Tensile strength of machine direction (kN/m)	22	
Elongation at peak of machine direction (%)	45	
CBR puncture resistance (N)	3750	
Geotextile properties	Bonded on the dimple side	Bonded on the flat side
Thickness at 2kPa (mm)	1.75	1.2
Tensile strength of machine direction (kN/m)	20	9.5
Pore size 090 (μm)	70	120
CBR puncture resistance (N)	3400	1600
Dynamic perforation cone drop (mm)	17	32

Table.2 The properties of Mercia Mudstone Clay

Plastic limit (%)	17.4
Optimal moisture content (%)	11.8
Liquid limit (%)	33.6